OTA ORTHOPAEDIC TRAUMA ASSOCIATION

OTA INTERNATIONAL
THE OPEN ACCESS JOURNAL OF ORTHOPAEDIC TRAUMA

OPEN

Comparing the volume of vascular intersection of two femoral neck fracture fixation implants using an *In silico* technique

Matthew D. Putnam, MD[a], Andrew Rau, MS, PE[b], Michael Frohbergh, PhD[b], Kevin Ong, PhD, PE[b], Michael Bushelow, MS[a,*], Michael Blauth, MD[a]

Background: Femoral neck fracture displacement with subsequent vascular disruption is one of the factors that contribute to trauma-induced avascular necrosis of the femoral head. Iatrogenic damage of the intraosseous arterial system during fixation of femoral neck fracture is another possible cause of avascular necrosis that is less well understood. Recently, Zhao et al (2017) reconstructed 3D structures of intraosseous blood supply and identified the epiphyseal and inferior retinacular arterial system to be important structures for maintaining the femoral head blood supply after femoral neck fracture. The authors therefore recommended placing implants centrally to reduce iatrogenic vascular injuries. Our in vitro study compared the spatial footprint of a traditional dynamic hip screw with an antirotation screw versus a newly developed hip screw with an integrated antirotation screw on intraosseous vasculature.

Methods: Three dimensional (3D) μCT angiograms of 9 cadaveric proximal femora were produced. Three segmented volumes—porous or cancellous bone, filled or cortical bone, and intraosseous vasculature—were converted to surface files. 3D in silico models of the fixation systems were sized and implanted in silico without visibility of the vascular maps. The volume of vasculature that overlapped with the devices was determined. The ratio of the vascular intersection to the comparator device was calculated, and the mean ratio was determined. A paired design, noninferiority test was used to compare the devices.

Results: Results indicate both significant ($P < 0.001$) superiority and noninferiority of the hip screw with an integrated antirotation screw when compared with a dynamic hip screw and antirotation screw for the volume of vasculature that overlapped with each device in the femoral neck.

Conclusions: Combining established methods of vascular visualization with newer methods enables an implant's impact on vascular intersection to be assessed in silico. This methodology suggests that when used for femoral neck fracture management, the new device intersects fewer blood vessels than the comparator. Comparative clinical studies are needed to investigate whether these findings correlate with the incidence of avascular necrosis and clinical outcomes.

Key Words: avascular necrosis, femoral neck fracture, femoral head, biomechanical study

1. Introduction

Avascular necrosis of the femoral head is most commonly associated with trauma and has a multifactorial etiology.[1] Among

factors under surgeons' control are the timing of surgery, quality of reduction, and implant choice and application.

Implants are mainly evaluated for their ability to achieve stable fracture fixation.[2,3] By contrast, the potential impact of implant dimensions, application mode, and intraosseous position on blood supply has not yet been systematically investigated to the best of our knowledge.

Zhao et al[4] used digital subtraction angiography and 3D μCT scans in 30 uninjured cadaveric femoral heads and 27 patients after femoral neck fractures before surgery to identify 3 main intraosseous vascular network structures with different contributions to the overall blood supply for anastomoses and calibers. The authors recommended to drill for and place implants close to the central region of the femoral head to avoid damage to the main afferent stems or major epiphyseal or metaphyseal branches of the intraosseous arterial network.

This cadaveric and in silico study was designed to determine differences between a commonly used "comparator" fixation device/method (dynamic hip screw [DHS] with antirotation screw) (Omega3 Compression Hip Screw, Asnis III Cannulated Screw, Stryker, Mahwah, NJ) and a newly developed "subject" fixation device [HS] (Femoral Neck System [HS], DePuy Synthes, West Chester, PA) on the volume of disrupted intraosseous vasculature. For both devices, the instructions for use suggest

positioning the main element in the center of the femoral neck and head in coronal and sagittal planes. We hypothesized that the HS device is noninferior to the DHS.

2. Materials and Methods

Fresh frozen cadaveric hemipelvises were procured from registered tissue foundations (institutional review board exemption). All donor tissues were screened for infectious disease. Nine femurs were acquired for the final study group and selected before the execution of any analysis of results, that is, no *post hoc* rejection of specimens was performed. Donors ranged from 46 to 75 years in age, with 5 female and 4 male donors. The study was given a non-human subject determination by an independent Institutional Review Board.

Before testing, the specimens were thawed at room temperature (~23°C) for approximately 48 hours. Each specimen was flushed with 1 L of saline (VWR International; Radnor, PA) using a source pressure of approximately 100 mm Hg. A tourniquet was applied to restrict blood flow to only the proximal portion of the tissue specimen, preferentially directing the flow into the deep femoral artery to feed the circumflex and retinacular arteries that supply blood to the femoral head. The system was then flushed with 0.5 L of saline at 37°C, followed by 1 L of heparinized 37°C saline (100 units heparin; Sigma Aldrich; St. Louis, MO). The femoral vasculature was then perfused with 2 L of 30% barium sulfate (Atlantic Equipment Engineers; Upper Saddle River, NJ) suspended in 5% gelatin (Sigma Aldrich; St. Louis, MO). The contrast suspension was injected using a syringe and manually maintained between 120 and 140 mm Hg. After perfusion, the specimen was placed into an ice water bath for at least 2 hours. The femur was then resected and cut for imaging.

The femoral head and neck were imaged using CT angiography techniques (μCT 80, Scanco Medical AG, Switzerland), which were similar to previous studies,[5,6] resulting in a maximum voxel size of 37 μm.[5,6] The reconstructed scans were imported into Simpleware ScanIP (Version N-2018.03-SP1, Synposis, Inc, Mountain View, CA) for postprocessing. Using voxel intensity (1900–8000 Hounsfield units), the scans were segmented into 2 primary volumes: a "filled" bone volume, which was bounded by the endosteal surface and the cut surface of the femur, and the intraosseous vasculature. Two regions of interest were identified based on regions selected in relevant publications[5,6]: Zone 1 was defined as the region proximal to the subcapital area while Zone 2 included the entirety of Zone 1 and extended distally to the narrowest portion of the femoral neck. The planes that defined the ends of the zones were perpendicular to the primary axis of the implants (ie, along the femoral neck axis).

The volume of the intraosseous vascular network, which overlapped the following 2 devices was evaluated: (1) the DHS with an outer diameter of 13 mm and accompanying, 6.5-mm diameter, 16-mm thread length, cancellous antirotation screw and (2) the newly developed HS, consisting of a nonthreaded 10-mm central bolt and an integrated 6.4-mm antirotation screw. Previous studies have reported localized trabecular bone damage adjacent to the implant during screw insertion [7.8], and in turn, the bone damage may disrupt the localized blood supply.[7–9] Therefore, to represent a worst-case scenario, each threaded component was modeled as a uniform cylinder with an outer diameter equal to the major diameter of the threaded portion of the component. To account for the potential disruption to the vasculature between the implanted components, the volume
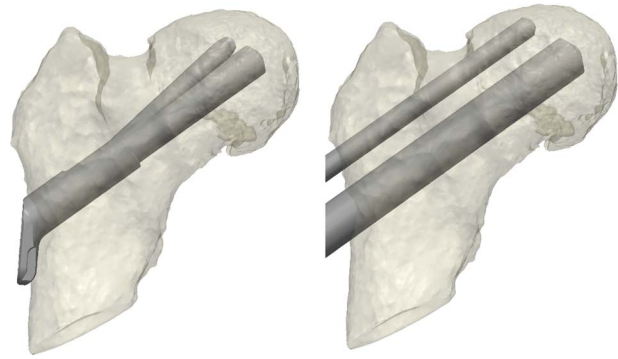

Figure 1. Representative images of the HS with integrated antirotation screw (left) and DHS with antirotation screw (right) device systems after in silico implantation into the 3D model.

between the components (intervening cancellous bone volume [ICBV]) was also considered. Device size and alignment within the specimen were selected based on the surgical guides for the HS and the DHS with antirotation screw, with consistent and clinically relevant placement of the devices across multiple anatomical specimens. All in silico implantations and size selections were performed using anatomical landmarks as references, but without the vascular map overlaid (Fig. 1).

The volumes of the vasculature that overlapped with the devices were determined for Zone 1 and Zone 2, both including and excluding the vasculature residing in the ICBV. Paired comparisons of the output metrics between the devices were performed for each donor to assess the differences in potential risk of vascular disruption. The ratio of the vascular intersection output metrics for the HS device to that of the DHS with antirotation screw for each donor specimen was calculated (paired comparison), and the mean ratio was determined across all donor specimens (Table 1, Fig. 2). A paired, noninferiority test was used to compare the overlapping vasculature-device volumes for the HS device and the DHS. A noninferiority design was selected because it is not an uncommon approach for designing clinical trials.[10] The null hypothesis stated that the ratio of overlapped volume for the HS device to that of the DHS device was greater than 120%. This margin was selected based on a conservative representation of the relative ratio in reported avascular necrosis (AVN) rates between predicate cancellous screws and sliding hip screws under observation from a femoral neck fracture clinical trial.[10,11] In this trial, a ratio of 177% between AVN rates between the cancellous and sliding hip screws was reported. Hence, the selection of 120% (compared with 177%) was considered to be a conservative noninferiority margin. Moreover, a noninferiority margin of 150% has been described as being commonly used for cardiovascular outcome studies, where the effects may be small.[10]

A mean ratio of 100%, mid-range coefficient of variation of 40%, and correlation of 90% were assumed. The statistical analysis was performed using SAS 9.4 (SAS, Cary NC).

3. Results

All specimens were evaluated with both the primary and antirotation screws, except for the DHS group where one specimen was evaluated with only the primary screw because of the anatomical size of the femur. The mean total bone volume, mean intraosseous vascular volume, and vascular volume–to–bone volume ratio were determined, and these volumes

TABLE 1

Description of Parameters of Interest for the Disruption Analysis

Quantity of Interest	Description
Volume of the surgical insertion pathway (VSIP)	Volume of the device components within the zone of interest (zones 1 or 2) in the femoral head
Intervening cancellous bone volume (ICBV)	Volume of the space between the device components (intervening cancellous bone) within the zone of interest in the femoral head
VSIP + ICBV	Total volume of the components and intervening cancellous bone within the zone of interest in the femoral head
VSIP and vessel intersection volume	Volume of vasculature, which overlaps with the device insertion pathway (VSIP)
ICBV and vessel intersection volume	Volume of vasculature, which overlaps with the intervening cancellous bone (ICBV)
VSIP + ICBV and vessel intersection volume	Total volume of vasculature, which overlaps with the device insertion pathway and intervening cancellous bone (VSIP + ICBV)
VSIP and vessel intersection volume ratio	Ratio of the "VSIP and vessel intersection volume" output parameter between the FNS device and the DHS with antirotation screw (FNS device:DHS with antirotation screw)
VSIP + ICBV and vessel intersection volume ratio	Ratio of the "VSIP + ICBV and vessel intersection volume" output parameter between the FNS device and the DHS with antirotation screw (FNS device:DHS with antirotation screw)

The 2 primary output metrics (ratios of vessel intersections for subject to the comparator) are shown in red in the bottom 2 rows.

and the ratio of the vascular-to-bone volumes were found to be comparable with previously published values.

Details on the volume of the surgical insertion path (VSIP), the ICBV, the sum of these volumes, and the results of the vessel intersections with these volumes for Zones 1 and 2 for the DHS and HS devices are listed in Table 2. Comparisons between the ratio of vessel intersection volume of the HS device to DHS are shown in Fig. 3.

Both superiority and noninferiority of the HS device for the DHS was demonstrated ($P < 0.001$) based on a noninferiority margin of 120% for both anatomical zones and both ratios ("VSIP and vessel intersection volume ratio" and "VSIP + ICBV and vessel intersection volume ratio"). The upper bound of the confidence intervals was found to be less than the margin of 120% and less than 100%. The results are summarized in Table 2.

4. Discussion

In this cadaveric study, applying μCT angiography and in silico modeling on 9 specimens, we compared 2 devices designed for fixation of femoral neck fractures to understand their impact on
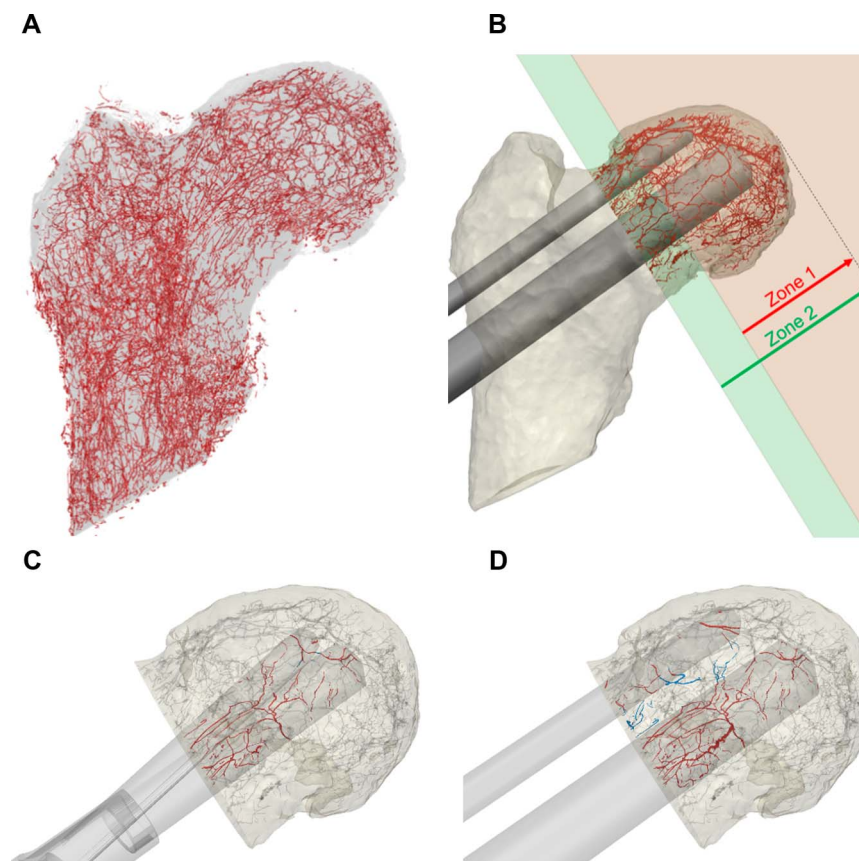
Figure 2. A, Maximum intensity anterior-posterior (AP) projection view of segmented blood vessels overlaid on the surfaces of the femoral head and neck. B, Zone 1 (red) and zone 2 (red + green) are defined by the subcapital and transcervical areas, respectively. These planes are defined to be approximately perpendicular to the axis of the implants and the axis of the femoral neck. C, Representative images of the HS device (right) and the DHS (left) showing vascular disruption in the femoral head. Vasculature that intersects directly with the device pathways (VSIP and vessel intersection volume) is shown in red; vasculature that intersects with the intervening cancellous bone (ICBV and vessel intersection volume) is shown in blue; and unaffected vasculature is shown in gray.

TABLE 2

Output Summary for all Specimens

Donor gender/age			F/75	M/61	F/48	M/61	F/70	F/60	F/69	M/51	M/66
BMI			16.8	41	27.0	29.0	27.0	19.5	40	23.8	19.0
Category	Device	Field (mm^3)									
Femoral head (Zone 1)	Anatomy	Intraosseous vessel volume	102	35.1	37.7	20.7	38.7	11.5	38.6	313	30.5
	HS device	Volume of the surgical insertion path (VSIP)	2391	2779	2172	2002	1578	1761	17,845	2003	1993
		Intervening cancellous bone volume (ICBV)	64.7	223	63.1	187	81.8	56.9	57.8	94.6	136
		VSIP + ICBV	2456	3001	2235	2189	1660	1818	1843	2098	2129
		VSIP and vessel intersection volume	3.4	4.8	5.9	0.6	2.4	1.2	2.9	18.1	4.5
		ICBV and vessel intersection volume	0.1	0.3	0.3	0.0	0.1	0.1	0.1	0.6	0.6
		VSIP + ICBV and vessel intersection volume	3.5	5.1	6.2	0.6	2.5	1.3	3.0	18.7	5.0
	DHS device	Volume of the surgical insertion path (VSIP)	3474	3976	2668	3046	2417	2685	2725	3047	3045
		Intervening cancellous bone volume (ICBV)	560	728	N/A*	311	162	180	189	208	205
		VSIP + ICBV	4034	4704	2668	3357	2579	2865	2914	3255	3250
		VSIP and vessel intersection volume	5.5	6.2	6.7	1.5	4.8	1.9	4.1	25.6	6.8
		ICBV and vessel intersection volume	0.5	0.9	N/A*	0.2	0.5	0.0	0.2	0.9	0.5
		VSIP + ICBV and vessel intersection volume	6.0	7.1	6.7	1.7	5.2	2.0	4.3	26.6	7.3
Femoral head (Zone 2)	Anatomy	Intraosseous vessel volume	131	81.9	71.2	60.6	105	42.9	144	517	86.1
	HS device	Volume of the surgical insertion path (VSIP)	3573	4256	3337	3955	3077	3557	2950	3064	3751
		Intervening cancellous bone volume (ICBV)	68.7	249	68.6	247	110	68.7	67.9	110	171
		VSIP + ICBV	3642	4505	3406	4202	3187	3626	3018	3174	3922
		VSIP and vessel intersection volume	5.4	5.7	9.7	1.3	6.8	2.9	4.0	32.6	5.7
		ICBV and vessel intersection volume	0.1	0.3	0.3	0.0	0.2	0.2	0.1	0.7	0.6
		VSIP + ICBV and vessel intersection volume	5.4	6.0	10.0	1.3	7.0	3.1	4.1	33.4	6.3
	DHS device	Volume of the surgical insertion path (VSIP)	5405	6227	4177	5975	4698	5563	4562	4674	5711
		Intervening cancellous bone volume (ICBV)	1009	1338	N/A*	649	336	400	329	332	409
		VSIP + ICBV	6413	7564	4177	6624	5033	5962	4891	5006	6120
		VSIP and vessel intersection volume	9.0	8.7	10.7	2.4	15.2	5.0	13.4	45.3	10.5
		ICBV and vessel intersection volume	1.1	1.3	N/A*	0.4	1.0	0.0	0.3	1.1	0.6
		VSIP + ICBV and vessel intersection volume	10.1	10.0	10.7	2.7	16.3	5.0	13.7	46.4	11.2

Summary results					
Zone	VSIP and vessel intersection volume geometric mean ratio (FNS/Omega3), % [95% CI]	*P*	VSIP + ICBV and vessel intersection volume geometric mean ratio (FNS/Omega3), % [95% CI]	*P*
1	63% [0%, 74%]	<0.001	64% [0%, 74%]	<0.001
2	55% [0%, 67%]	<0.001	56% [0%, 68%]	<0.001

* Owing to anatomical sizing and limitations, no antirotation screw was used for this in silico implantation.

the intraosseous vascular network of the femoral neck and head and the potential risks of iatrogenic disruption of the intraosseous blood supply. Both device systems consisted of a central load carrier and an antirotation screw to withstand rotational forces on the femoral head.

Over the past 50 years, many vascular perfusion studies of cadaveric tissue have been performed,[12–17] including several with specific application to the femoral head and neck.[4–6,18–22] Femoral head vasculature has been mapped using CT angiography and can be performed using BaSO4, a contract agent, that is radiographically visible. Using these types of techniques, researchers have been able to quantify the length, diameter, and volume of vasculature in the femoral head. Furthermore, the vasculature of the femoral head has been mapped using CT angiography.[4–6,21,22]

Researchers have quantified measurements of length, diameter, and volume of vasculature in the femoral head.[4–6] Zhao et al[4] generated vascular maps of 30 uninjured cadaveric femoral heads and observed the presence of more main epiphyseal arteries and fewer anastomoses in the peripheral regions of the intraosseous vascular as opposed to the central regions. Although those researchers did not quantify how much of the vasculature may be affected, they performed qualitative visual evaluations of internal fixation implant positioning and hypothesized that the peripheral regions of the intraosseous system were more vulnerable to the damaging effects of fixation surgery than the central region.

The average vascular and bone volumes as determined in this in silico study are comparable with those provided in the literature.[5,6] The parameters from Zone 2 as defined in this study are more similar to those reported by Qiu et al in 2018[5] and represent the best agreement between the in silico study results and the published literature. The 2016 study by the same group[6] reported much larger vascular volumes and bone volumes than the 2018 work,[5] which could be indicative of high patient variability, subjectivity when defining the zone of interest, or improvement of the perfusion method. Comparing the average ratio of vascular volume to bone volume from the 2018 data published by Qiu et al, which ranged from 0.04% to 0.87%,[5] as compared with the averages from this study: 0.5% and 0.9% for Zone 1 and Zone 2, respectively, supports the idea that vascularity is variable and that our specimens had variability similar to that observed in the study by Qiu et al. Given the variability in bone and vascular volumes reported within a single research group, the volumes used for the in silico calculations are similar to existing data. Importantly, ratios of the intersected vascular volumes between the HS device and the DHS with antirotation screw demonstrated both superiority and non-inferiority of the HS device for both anatomical zones and both intersected vascular volume ratios that were examined in the study.

Trauma-induced AVN of the femoral head represents a common sequelae after femoral neck fractures and has a multifactorial etiology. Zhao et al[4] confirmed clinicians' shared
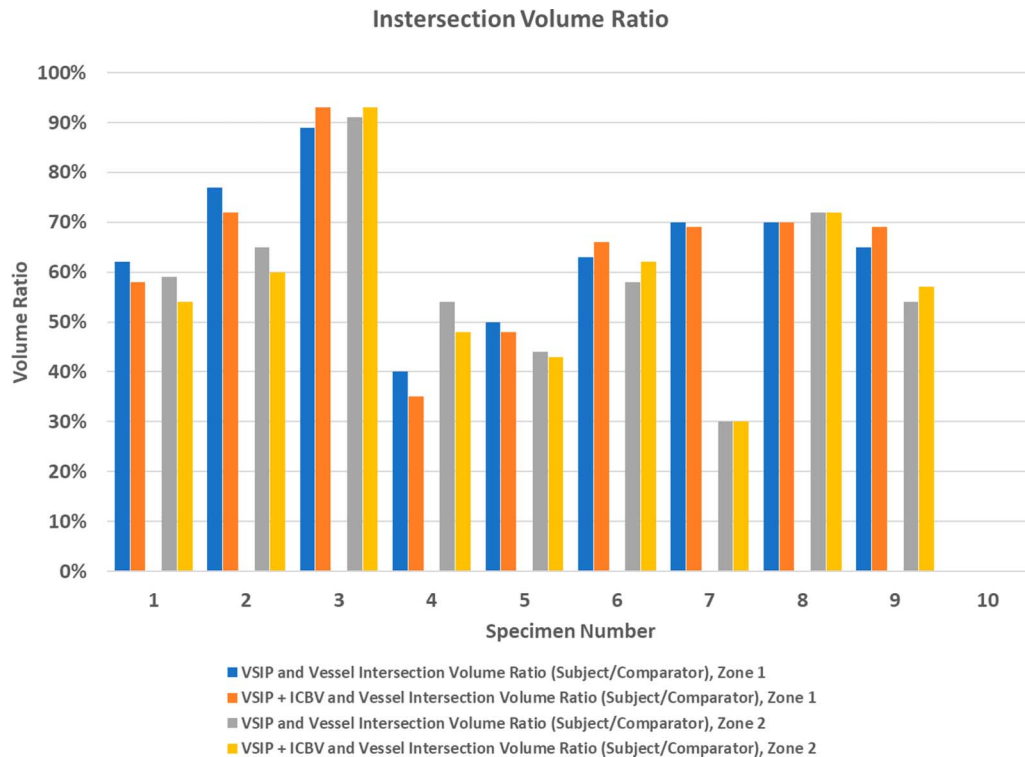
Instersection Volume Ratio

Figure 3. Graphical representation of the ratio of vessel intersection volume of the HS device to the DHS.

belief that vascular damage directly correlates with fracture displacement/instability in 27 femoral neck fracture patients with in vivo digital subtraction angiography data. Of course, many factors, such as reduction maneuvers or the implants chosen to stabilize the fracture, might affect residual blood supply to the femoral head. Recognizing that surgeons have a role in preserving femoral head blood supply, Zhao et al considered the possibility that implants may need to be placed closer to the central region of the femoral head based on the "3-D anatomic evidence of intraosseous arterial distribution of the femoral head and the high frequency with which the inferior retinacular arteries remained patent after femoral neck fracture."

It was noted earlier that construct "strength" measures have often been the primary design goal of fixation devices. It should be noted that the quality of rotational and angular fixation of these 2 devices has been previously biomechanically compared and have been found to provide adequate and comparable support to femoral neck fractures.[23] At some point, strength gains from design change may not be meaningful, but other design elements may offer relative benefits. In the context of pursuing the Hippocratic admonition, one may speculate that the bone and residual vasculature volume that is disrupted by drilling and placing stabilizing implants into the head-neck fragment has the potential to additionally increase the extent and/or risk of AVN.[24,25] In that sense, the HS device performed significantly better than the DHS as determined by fewer vascular intersections. It remains to be seen whether corresponding results can be generated in clinical studies and lead to clinically relevant differences in either AVN rates or clinical outcomes.

There are limitations of this study. The in silico placement of the devices was performed by a small group of experts. Analysis of a larger, more anatomically diverse sample group might have yielded different results. In addition, based on the design, it is not possible to draw direct conclusions regarding the frequency and extent of AVN in real-world scenarios.

Combining established methods of vascular visualization with newer methods enables an implant's impact on vascular intersection to be assessed in silico. This methodology suggests that when used for femoral neck fracture management, the HS device intersects fewer blood vessels than the DHS with antirotation screw. Comparative clinical studies are needed to investigate whether these findings correlate with the incidence of AVN and clinical outcomes.

References

1. Bachiller FG, Caballer AP, Portal LF. Avascular necrosis of the femoral head after femoral neck fracture. *Clin Orthop Relat Res.* 2002;399: 87–109.
2. Holmberg S, Kalen R, Thorngren KG. Treatment and outcome of femoral neck fractures. An analysis of 2418 patients admitted from their own homes. *Clin Orthop Relat Res.* 1987;218:42–52.
3. McCutchen JW, Carnesale PG. Comparison of fixation in the treatment of femoral neck fractures. *Clin Orthop Relat Res.* 1982;171:44–50.
4. Zhao D, Qiu X, Wang B, et al. Epiphyseal arterial network and inferior retinacular artery seem critical to femoral head perfusion in adults with femoral neck fractures. *Clin Orthop Relat Res.* 2017;475:2011–2023.
5. Qiu X, Cheng LL, Wang BJ, et al. Micro perfusion and quantitative analysis of the femoral head intraosseous artery. *Orthop Surg.* 2018;10: 69–74.
6. Qiu X, Shi X, Ouyang J, et al. A method to quantify and visualize femoral head intraosseous arteries by micro-CT. *J Anat.* 2016;229:326–333.
7. Ryan MK, Mohtar AA, Cleek TM, et al. Time-elapsed screw insertion with microCT imaging. *J Biomech.* 2016;49:295–301.
8. Steiner JA, Ferguson SJ, van Lenthe GH. Screw insertion in trabecular bone causes peri-implant bone damage. *Med Eng Phys.* 2016;38:417–422.
9. Marenzana M, Arnett TR. The key role of the blood supply to bone. *Bone Res.* 2013;1:203–215.
10. *Non-Inferiority Clinical Trials to Establish Effectiveness: Guidance for Industry.* 2016. Rockville, MD: U.S. Department of Health and Human

Services, Food and Drug Administration, Center for Drug Evaluation and Research (CDER), Center for Biologics Evaluation and Research (CBER).

11. FAITH Investigators. Fracture fixation in the operative management of hip fractures (FAITH): an international, multicentre, randomised controlled trial. *Lancet*. 2017;389:1519–1527.

12. Brooks CH, Revell WJ, Heatley FW. Vascularity of the humeral head after proximal humeral fractures. An anatomical cadaver study. *J Bone Joint Surg Br*. 1993;75:132–136.

13. Carey JN, Minneti M, Leland HA, et al. Perfused fresh cadavers: method for application to surgical simulation. *Am J Surg*. 2015;210:179–187.

14. Carey JN, Rommer E, Sheckter C, et al. Simulation of plastic surgery and microvascular procedures using perfused fresh human cadavers. *J Plast Reconstr Aesthet Surg*. 2014;67:e42-e48.

15. Claffey TJ. Avascular necrosis of the femoral head. An anatomical study. *J Bone Joint Surg Br*. 1960;42-B:802–809.

16. Han H, Tao W, Zhang M. The dural entrance of cerebral bridging veins into the superior sagittal sinus: an anatomical comparison between cadavers and digital subtraction angiography. *Neuroradiology*. 2007;49:169–175.

17. Meyer C, Alt V, Hassanin H, et al. The arteries of the humeral head and their relevance in fracture treatment. *Surg Radiol Anat*. 2005;27:232–237.

18. Kalhor M, Beck M, Huff TW, et al. Capsular and pericapsular contributions to acetabular and femoral head perfusion. *J Bone Joint Surg Am*. 2009;91:409–418.

19. Kalhor M, Horowitz K, Gharehdaghi J, et al. Anatomic variations in femoral head circulation. *Hip Int*. 2012;22:307–312.

20. Yue JJ, Wilber JH, Lipuma JP, et al. Posterior hip dislocations: a cadaveric angiographic study. *J Orthop Trauma*. 1996;10:447–454.

21. Zlotorowicz M, Czubak J, Caban A, et al. The blood supply to the femoral head after posterior fracture/dislocation of the hip, assessed by CT angiography. *Bone Joint J*. 2013;95-B:1453–1457.

22. Zlotorowicz M, Czubak J, Kozinski P, et al. Imaging the vascularisation of the femoral head by CT angiography. *J Bone Joint Surg Br*. 2012;94:1176–1179.

23. Stoffel K, Zderic I, Gras F, et al. Biomechanical evaluation of the femoral neck system in unstable Pauwels III femoral neck fractures: a comparison with the dynamic hip screw and cannulated screws. *J Orthop Trauma*. 2017;31:131–137.

24. Abbasi K. First do no harm: the impossible oath. *BMJ*. 2019;366:l4734.

25. Restas S. Response to "first do no harm: the impossible oath". *BMJ*. 2019;366:l4734.